International Journal of Minerals, Metallurgy and Materials
Volume 22, Number 4, April 2015, Page 363
DOI: 10.1007/s12613-015-1081-3

Comparison of kinetic models for isothermal CO_2 gasification of coal char–biomass char blended char

Hai-bin Zuo[1)], *Wei-wei Geng*[1)], *Jian-liang Zhang*[2)], *and Guang-wei Wang*[2)]

1) State Key Laboratory of Advanced Metallurgy, University of Science and Technology Beijing, Beijing 100083, China
2) School of Metallurgical and Ecological Engineering, University of Science and Technology Beijing, Beijing 100083, China
(Received: 26 February 2014; revised: 5 May 2014; accepted: 8 May 2014)

Abstract: This study investigated the isothermal gasification reactivity of biomass char (BC) and coal char (CC) blended at mass ratios of 1:3, 1:1, and 3:1 via isothermal thermogravimetric analysis (TGA) at 900, 950, and 1000°C under CO_2. With an increase in BC blending ratio, there were an increase in gasification rate and a shortening of gasification time. This could be attributed to the high specific surface area of BC and the high uniformity of carbon structures in CC when compared to those in BC. Three representative gas–solid kinetic models, namely, the volumetric model (VM), grain model (GM), and random pore model (RPM), were applied to describe the reaction behavior of the char. Among them, the RPM model was considered the best model to describe the reactivity of the char gasification reaction. The activation energy of BC and CC isothermal gasification as determined using the RPM model was found to be 126.7 kJ/mol and 210.2 kJ/mol, respectively. The activation energy was minimum (123.1 kJ/mol) for the BC blending ratio of 75%. Synergistic effect manifested at all mass ratios of the blended char, which increased with the gasification temperature.

Keywords: ironmaking; coal char; biomass; gasification; kinetic models; synergistic effect

1. Introduction

Lately, gas-based shaft furnace direct reduction technology has developed rapidly worldwide owing to its unique advantages, including quicker reduction, flexible product quality, highly automatic, low energy consumption, and low environmental impact [1]. However, the vast availability of coal and lack of natural gas in China's energy structure is the bottleneck limiting its development in China. Biomass is widely considered as a potential substitute for fossil fuels, as it is carbon-rich, neutral, renewable, and environmentally friendly [2–3]. Given the consideration of the current situation of China rich in non-coking coal and biomass, the co-gasification of biomass and coal can be considered as potential feedstock for the supply of reducing gas used in direct reduction iron-making technology by gasification. Therefore, co-gasified coal and biomass are not only beneficial for the development of gas-based shaft furnace technology in China, but also contribute to the reduction of the fossil fuel dependency and CO_2 emissions [4].

Until now, several studies have analyzed the co-gasification of biomass and coal [5–10]. Most studies have focused on the influence of the co-gasification of raw biomass and coal on the gas compositions, tar cracking, output and gas beating value of gas, gas yield, and gas efficiency. However, to the best of our knowledge, studies on the co-gasification of biomass char and coal char have been rarely reported in the literature. Gasification can be divided into two main stages, namely, pyrolysis and char gasification. Among these, char gasification is the rate-determining step of the gasification process [11–13]. The differences in the gasification characteristics of biomass char and coal char will result in certain difficulties in terms of the design and run of gasification reactors. In this study, we have performed thermogravimetric analysis (TGA) to investigate the gasification kinetics of biomass char and coal char, and their blends. In addition, isothermal experiments have been performed, and three mathematical models, including the volumetric model (VM) [14], grain model (GM) [15], and

Corresponding author: Hai-bin Zuo E-mail: zuohaibin@ustb.edu.cn

random pore model (RPM) [16], have been used to determine the kinetic parameters, in order to develop the basic theory supporting biomass char and coal char blended gasification.

2. Kinetic models for char gasification reaction

In order to develop the kinetic model of char gasification, the gasification reaction rate (r) was considered by the following rate equation [17]:

$$r = \frac{\mathrm{d}X}{\mathrm{d}t} = k\left(P_{\mathrm{CO_2}}, T\right) f\left(X\right) \tag{1}$$

where k is the reaction rate constant, which includes the effect of temperature (T) and the effect of gasifying agent partial pressure ($P_{\mathrm{CO_2}}$); X is the carbon conversion ratio; $f\left(X\right)$ is a kinetic-model dependent function, which can describe the changes in the physical or chemical properties of the sample during gasification; t is the time. Assuming that the partial pressure of CO_2 remains constant during the process, the reaction rate constant can be expressed using the Arrhenius equation, as follows:

$$k = k_0 \mathrm{e}^{-E/RT} \tag{2}$$

where k_0, E, and R are the pre-exponential factor, activation energy, and universal gas constant (8.314 J/mol·K), respectively.

Furthermore, three models were implemented to interpret the experimental results, namely, VM, GM, and RPM, as they have a theoretical basis and involve fewer parameters. These models give different formulations of the term $f\left(X\right)$.

The VM assumes that a homogeneous reaction occurs throughout the char bed and that it results in a linear decrease in the reaction surface area with conversion [14]. The overall reaction rate is given by

$$\frac{\mathrm{d}X}{\mathrm{d}t} = k_{\mathrm{VM}}(1-X) \tag{3}$$

The GM considers that the gasifying agents react on the surface of the non-porous grains or in pore surfaces within the solid [15]. According to different assumptions, the reaction rates in the regime of chemical control can be expressed as

$$\frac{\mathrm{d}X}{\mathrm{d}t} = k_{\mathrm{GM}}(1-X)^{2/3} \tag{4}$$

The RPM considers the overlapping of pore surfaces, which results in the reduction of surface area available for the reaction [16]. The general rate equation for this model is

$$\frac{\mathrm{d}X}{\mathrm{d}t} = k_{\mathrm{RPM}}\left(1-X\right)\sqrt{1-\psi\ln\left(1-X\right)} \tag{5}$$

This model can predict a maximum for the reactivity during the reaction, as it considers the competing effects of pore growth during the initial stages of gasification, and the destruction of the pores due to the coalescence of neighboring pores during the reaction. The RPM contains two parameters, ψ, which is related to the initial pore structure of the char sample ($X = 0$) and the reaction rate constant, k.

$$\psi = \frac{4\pi L_0\left(1-\varepsilon_0\right)}{S_0^2} \tag{6}$$

where S_0, L_0, and ε_0 represent the pore surface area, pore length, and solid porosity, respectively.

The nonlinear least-squares method was employed to fit the experimental data of dX/dt vs. X to the three models, The following equation was used to determine the kinetics parameters (k_{VM}, k_{GM}, k_{RPM}, and ψ) by employing nonlinear least-squares fitting methods, which minimizes the objective function OF:

$$\mathrm{OF} = \sum_{i=1}^{n}\left[\frac{\left(\frac{\mathrm{d}X}{\mathrm{d}t}\right)_{\mathrm{exp},i} - \left(\frac{\mathrm{d}X}{\mathrm{d}t}\right)_{\mathrm{model},i}}{\left(\frac{\mathrm{d}X}{\mathrm{d}t}\right)_{\mathrm{exp},i}}\right]^2 \tag{7}$$

where $\left(\frac{\mathrm{d}X}{\mathrm{d}t}\right)_{\mathrm{exp},i}$ is the experimental data, $\left(\frac{\mathrm{d}X}{\mathrm{d}t}\right)_{\mathrm{model},i}$ is the value calculated by the model, and n is the number of data points.

3. Experimental

3.1. Char preparation

The raw materials used in this study are scraps of sawmill woody biomass (BS) and Jizhong anthracite (JZ). Biomass char (BC) and coal char (CC) were made using a tube type resistance furnace SK13-12 (12kW, 1350°C, heating chamber ϕ120 mm × 250 mm), followed by the carbonization of BS and JZ at 1100°C with a hold time of 60 min. The carbonization process was performed under protected N_2 atmosphere (120 mL/min). The char samples thus obtained were ground and sieved to a size of <200 μm. Subsequently, BC and CC were thoroughly mixed at mass ratios of 1:3, 1:1, and 3:1 using an agate mortar for 10 min. The results of proximate and ultimate analyses of the samples are listed in Table 1, on the basis of the ASTM D5373 criterion and GB212—91/GB212—84 criterion, respectively. The specific surface area of the sample was analyzed by Autosorb-iQ-C automated physisorption and chemisorption analyzer.

Table 1. Proximate and ultimate analyses of the samples wt%

Sample	Proximate analysis			Ultimate analysis				
	FC_d	A_d	V_d	C	H	O	N	S
BS	16.39	0.45	83.16	48.04	5.6	39.77	0.37	0.06
JZ	70.43	14.69	14.88	75.23	2.5	1.01	0.93	0.85
BC	93.37	1.579	5.05	96.68	0.25	0.16	1.01	0.06
CC	83.37	15.58	1.05	84.29	0.23	0.25	0.78	0.80

Note: FC_d, V_d, and A_d are solid carbon, volatile, and ash content, respectively.

3.2. Gasification tests

TGA tests were carried out on a WCT-3 thermal balance to obtain the mass loss curve at atmospheric pressure. In the experiments of char gasification with carbon dioxide, the reaction temperature was 900, 950, and 1000°C. For the analysis, approximately 5 mg of the sample was placed in an alumina crucible (ϕ3 mm × 1.5 mm). Char gasification was performed by the following procedure show in Table 2. It was important to ensure that the experiment has good reproducibility. Thus, each test was repeated at least thrice before a final result was ascertained.

Table 2. Procedure adopted for the char gasification

Step	Description	Stage
1	Flow of pure Ar gas (100 mL/min)	Initial
2	Ramp to $T_{isothermal}$ with 20°C/min	Heating
3	Flow of pure Ar gas for 5 min at $T_{isothermal}$	Isothermal
4	Shift from pure Ar to CO_2 (100 mL/min, 99.999%)	Isothermal
5	Hold at $T_{isothermal}$ for 2 h	Isothermal
6	Cool to room temperature	Cooling

The carbon conversion ratio (X) was calculated by the following equation:

$$X = \frac{m_0 - m_t}{m_0 - m_\infty} \tag{8}$$

where m_0 denotes the sample mass at the start of the gasification, m_t is the sample mass at the gasification time t, and m_∞ is the mass of ash remaining after complete gasification.

An additive model was used to evaluate the synergy during the CO_2 co-gasification of the blended char. According to the additive model, the co-gasification characteristics for all the blending conditions are deducible from the gasification characteristics of each pure sample. The theoretical and experimental $\frac{dX}{dt}$ curves of the char were compared in order to determine the component of the blended char that interacted during the gasification process. The theoretical $\frac{dX}{dt}$ curves of the blends were calculated according to the additive rule of blends, as follows:

$$\left(\frac{dX}{dt}\right)_{Cal} = F_1\left(\frac{dX}{dt}\right)_{BC} + F_2\left(\frac{dX}{dt}\right)_{CC} \tag{9}$$

where $\left(\frac{dX}{dt}\right)_{BC}$ and $\left(\frac{dX}{dt}\right)_{CC}$ are the reaction rates of the BC and CC, and F_1 and F_2 are the mass proportions of BC and CC in the blended char, respectively.

The theoretical blended char reaction rate constant by RPM $(k_{RPM})_{Cal}$ was calculated by the following function:

$$(k_{RPM})_{Cal} = F_1(k_{RPM})_{BC} + F_2(k_{RPM})_{CC} \tag{10}$$

where $(k_{RPM})_{BC}$ and $(k_{RPM})_{CC}$ are the RPM reaction rate constants of BC and CC, respectively.

The theoretical blended char gasification activation energy $(E)_{Cal}$ can be calculated according to the mass proportions of BC and CC. The calculation function is as follows:

$$E_{Cal} = F_1E_{BC} + F_2E_{CC} \tag{11}$$

where E_{BC} and E_{CC} are the gasification activation energies of BC and CC, respectively.

4. Results and discussion

4.1. Structural characteristics of the char

The scanning electron microscope (SEM) images of BC and CC presented in Fig. 1 indicate that the BC particles have a loose lamellar structure with thin walls (approximately 1–5 μm), which is probably the broken honeycomb structure after the loss of substantial volatiles in biomass. On the other hand, the CC particles exhibit an irregular shape and relatively compact structure. Therefore, under the same volume condition, the specific surface area of BC should be higher than that of CC. The specific surface area of BC is 73.2 m^2/g, while that of the CC char is much lower (7.07 m^2/g). This results in the lower reactivity of CC compared to that of the BC, which is in accordance with the study reported by Yuan *et al.* [8,18] that the specific surface area has a great influence on the gasification reactivity. Fig. 2 shows

the particle size distribution of BC and CC. As is seen, the particle size of CC ranges from 2.5 to 130 μm and mainly concentrates on 8–80 μm. On the other hand, the particle size of BC ranges from 9 to 130 μm and mainly concentrates on 20–74 μm. The degree of concentration of BC is superior to CC.

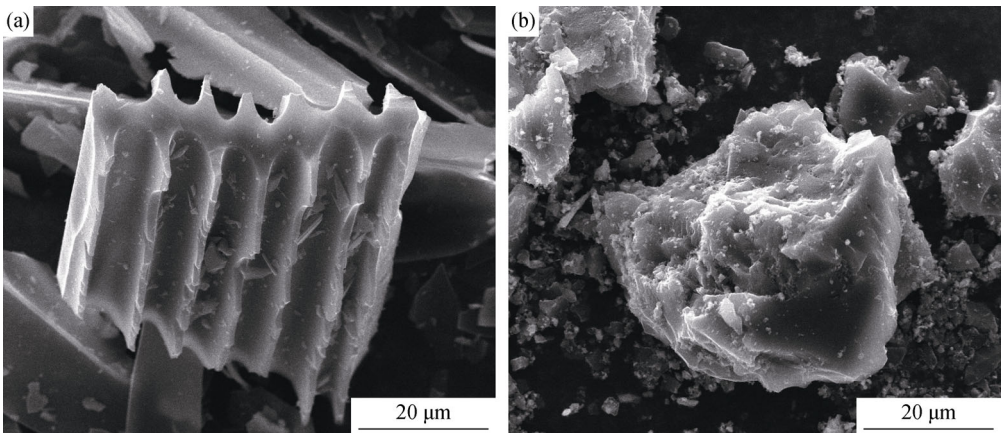

Fig. 1. SEM images of biomass char particles (a) and coal char particles (b).

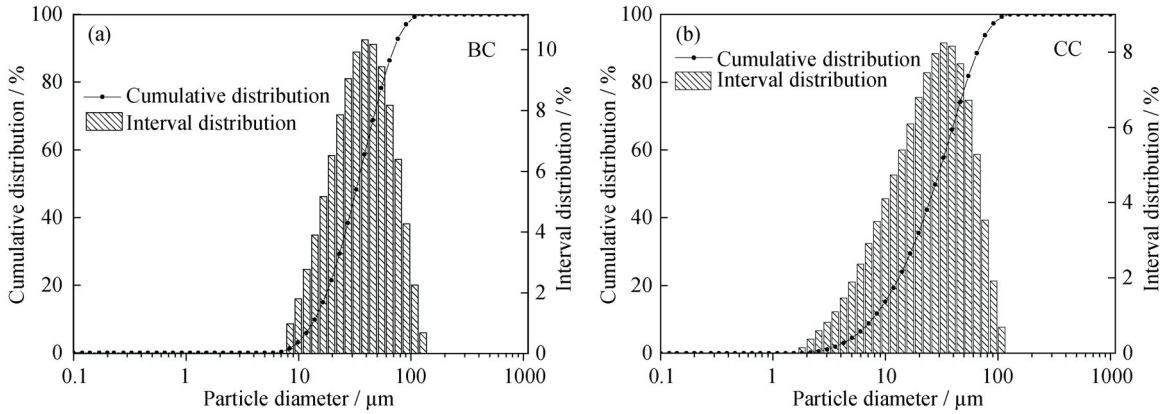

Fig. 2. Size distribution of the biomass char (a) and coal char (b).

4.2. Gasification reactivity of the char

Fig. 3 shows the carbon conversion ratios over time and the differential thermal gravity (DTG) curves of the BC/CC blended char during isothermal gasification at 950°C under CO_2. As can be seen from Fig. 3(a), CC has the lowest gasification rate, and the gasification rate increases with an increase in the BC share due to the high reactivity of BC. Moreover, Fig. 3(b) reveals that gasification peak value (R_m) of the BC/CC blended char occurred relatively earlier than CC or BC probably due to the synergetic effect of the BC/CC blended char [9]. Fig. 4(a) shows that total gasification time (t_{total}) of CC and BC/CC at mass ratios of 1:3, 1:1, and 3:1 are almost 3.6, 3.4, 2.4, and 1.6 times higher than that of BC. This indicates that BC could highly promote the char reactivity. With an increase in BC proportion, t_{total} decreases and R_m increases (Fig. 4(a)). It may be attributed to the following two reasons: (1) the reaction surface of the char increased due to the increase in BC proportion, which may partly account for the gasification rate of CC lower than the blended char; (2) the other reason is the intrinsic chemical structure of the char. According to the Raman shift of BC and CC (Fig. 4(b)), as determined from Raman analysis, the peak appearing at approximately 1350 cm^{-1} and 1580 cm^{-1} can be attributed to the D and G band, respectively, corresponding to the amorphous carbon structures and C=C bonds of graphite crystals. The V band, whose intensity is denoted by I_V, lies at the valley of about 1500 cm^{-1} between the D and G bands. The intensities of D and G bands can be denoted as I_D and I_G, respectively. The uniformity of the carbon structures can be determined from the I_V/I_G ratio, the decrease of which is related to the increase in the uniformity of carbon structures [19]. In general, the gasification rate decreases with an increase in uniformity. As can be observed from Fig. 4(b), the I_V/I_G values of BC and CC are 0.522 and 0.473, respectively. It proves that the gasification rate of the BC is higher than CC.

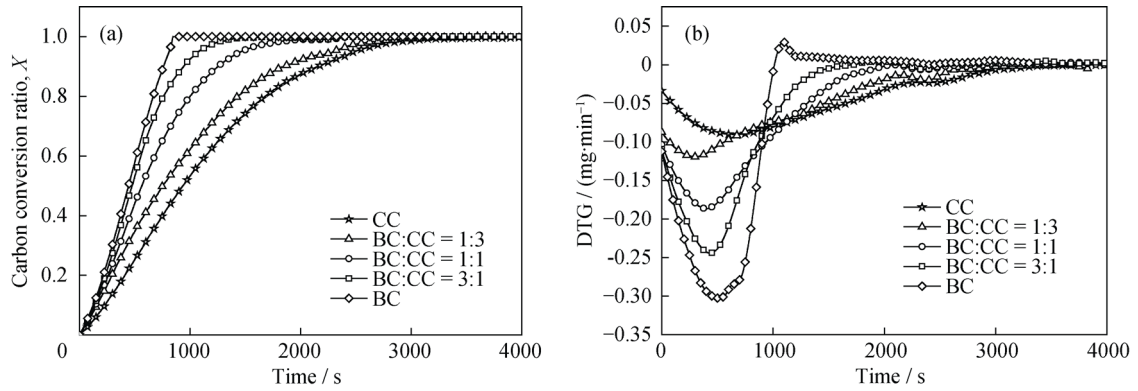

Fig. 3. (a) Carbon conversion ratio (X) of the BC/CC blended char plotted as a function of reaction time (t); (b) DTG curves of the BC/CC blended char at 950°C.

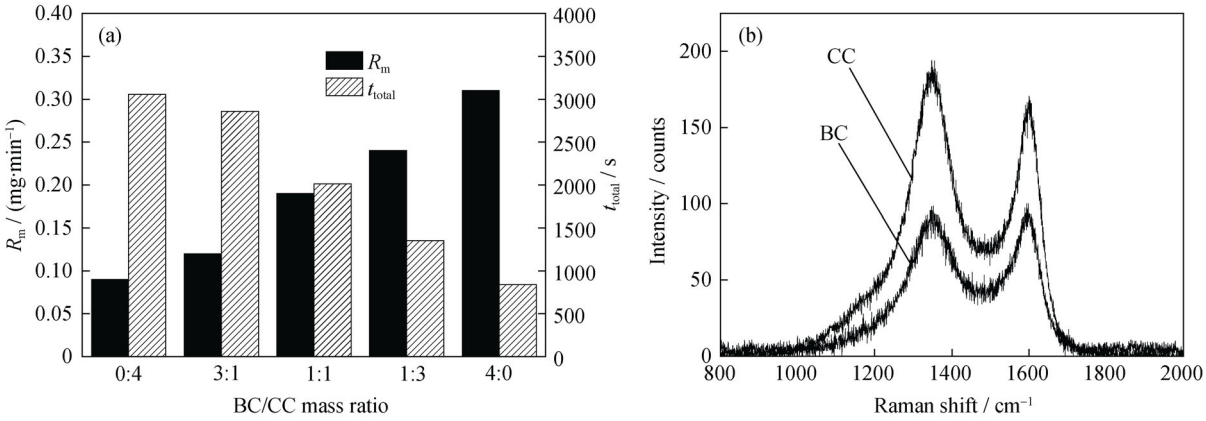

Fig. 4. (a) t_{total} and R_m of the BC/CC blended char at different mass ratios; (b) Raman shift of BC and CC.

4.3. Kinetic analysis

The applicability of VM, GM, and RPM kinetic models to describe the gasification rate of char at various temperatures and mass ratios are presented in Figs. 5(a)–5(e). The kinetic parameters of the applied models and the regression coefficients (R^2) are summarized in Table 3. On the basis of the curve fitting results, it can be concluded that the RPM model could best describe the gasification process at all implemented temperatures than those of the VM and GM. This can be attributed to the fact that the VM and GM kinetic models cannot explain the gasification reaction rate (r) along with the change of carbon conversion ratio in the first peak followed by a gradual declination in the trend. On the other hand, the RPM kinetic model explains it as the growth of reaction surfaces associated with the pores and the loss of these surfaces as they progressively collapse by intersection [16]. These results are in good agreement with the previous studies [19–20], which concluded that the random pore model is more appropriate in explaining the biomass char and coal char gasification reaction.

During gasification, mass transfer (gas diffusion) takes place inside the bed of particles as well as inside the pores of the single particle. Kim *et al.* [21] confirmed that the mass transfer can be negligible and chemical reaction is the rate controlling step when the reaction rate is lower than 0.0082 s^{-1}. In this study, the maximum reaction rate of gasification (r_{max}) was 0.0015 s^{-1} in the case of the absence of CC and a gasification temperature of 1000°C (Fig. 5(f)), far less than 0.0082 s^{-1}. Therefore, the co-gasification reaction of the blended char is controlled via the chemical reaction.

Fig. 6 shows the straight line fit of $\ln k_{RPM}$ versus $1/T$, which could provide the activation energy E and pre-exponential factor k_0 listed in Table 3. The activation energy of CC, as obtained by using the RPM model, was about 210.2 kJ/mol, which is closer to the values obtained by using the VM and GM models (200.4 kJ/mol and 209.8 kJ/mol, respectively). The minimum activation energy of the blended char using all the models was about 130 kJ/mol at a BC/CC mass ratio of 3:1. Accordingly, the BC blending ratio of 75% is considered optimum to enhance the gasification efficiency and carbon conversion rate. The activation energy of BC obtained by an average value of three kinetic models was about 131.6 kJ/mol, which is consistent with the values

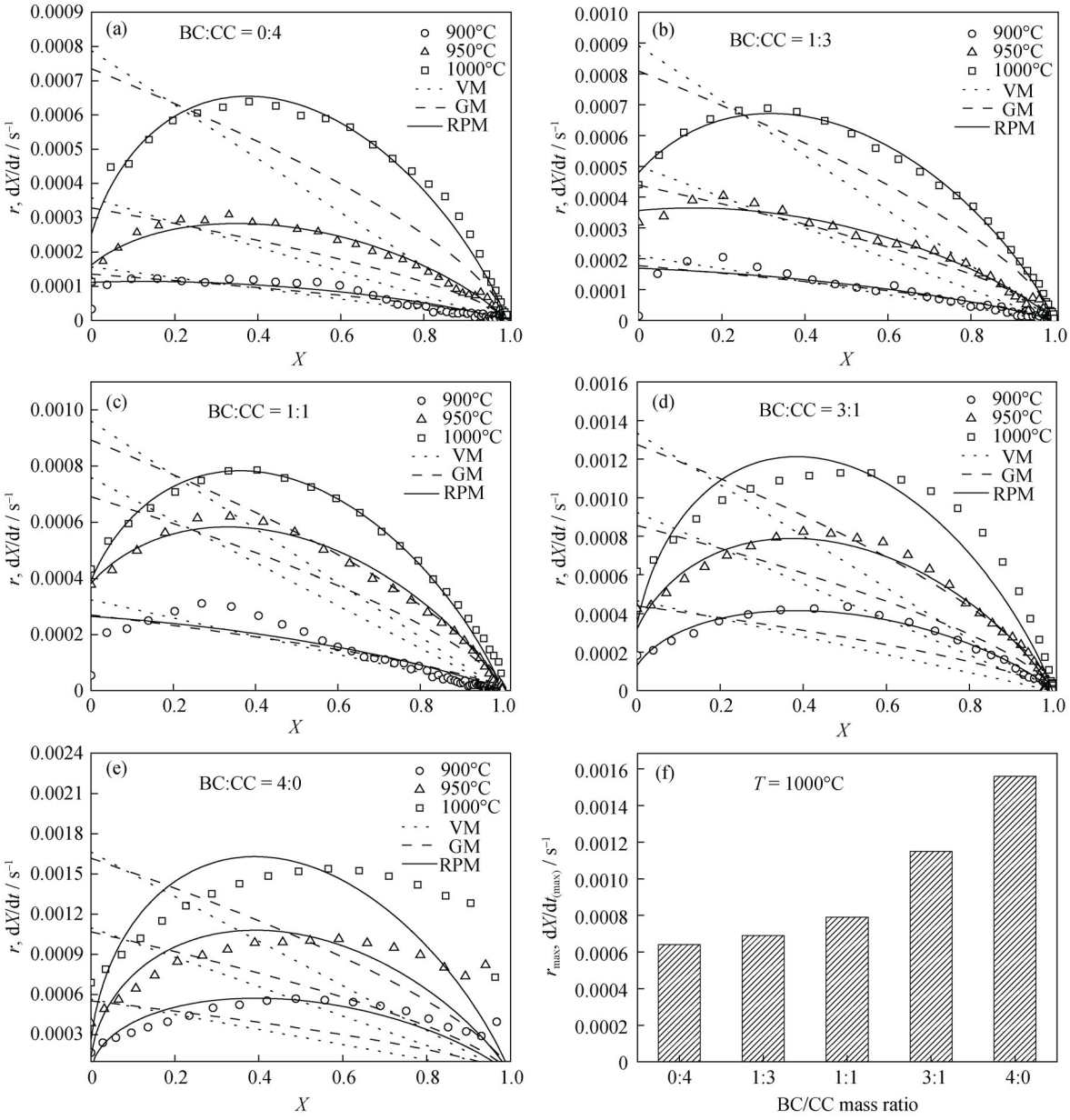

Fig. 5. (a)–(e) Gasification reaction rates (r) of the BC/CC blended char at different mass ratios and fitting curves of VM, GM and RPM; (f) maximum gasification reaction rate (r_{max}) of the BC/CC blended char at different mass ratios.

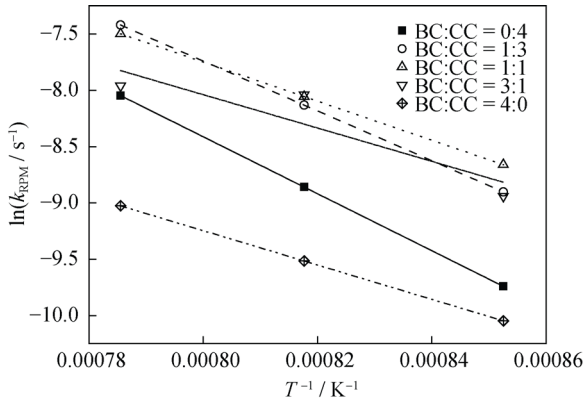

Fig. 6. Arrhenius curves of char gasification reactions.

reported in previous works [18,20,22]. According to Blasi [23], the activation energy of biomass char is typically within the range of 80.3–261 kJ/mol. As shown in Table 3, the activation energy of the blended char obtained by all the kinetic models decreased with an increase in the amount of BC in the blended char. Furthermore, with the increase of BC in the blended char, the regression coefficients (R^2) decline slightly. Besides, the RPM model could not satisfactorily fit the data of the BC sample due to the high value of ψ at a BC/CC mass ratio of 4:0. As mentioned earlier, BC has extremely high reactivity, probably because of the high specific surface area and lower crystal uniformity. This could

probably be the reason why the reactivity of BC could not be described properly with the models adopted in this work, since these models take into account only the structural changes during the gasification process. Therefore, the specific promoting effect of BC in gasification needs further discussion.

Table 3. Kinetic parameters of the chars at three temperatures for RPM, GM, and VM

BC:CC	VM			GM			RPM			
	E / (kJ·mol^{-1})	k_0 / s^{-1}	R^2	E / (kJ·mol^{-1})	k_0 / s^{-1}	R^2	E / (kJ·mol^{-1})	k_0 / s^{-1}	ψ	R^2
0:4	200.4	1.31×10^5	0.7864	209.8	2.98×10^5	0.6002	210.2	1.35×10^5	19.43	0.9797
1:3	179.7	2.24×10^4	0.8989	188.5	4.57×10^4	0.7794	183.8	2.10×10^4	4.47	0.9713
1:1	135.8	3.97×10^2	0.7566	149.6	1.37×10^3	0.5460	144.3	4.62×10^2	9.79	0.9102
3:1	130.3	3.11×10^2	0.8128	132.1	3.47×10^3	0.6940	123.1	4.46×10	48.94	0.9097
4:0	134.3	5.57×10^2	0.6316	134.0	5.31×10^3	0.7387	126.7	1.90×10	1017.46	0.8424

The blended char reaction rate constant by RPM (k_{RPM}), as determined from the experiment and calculation, are shown in Fig. 7(a). The calculated value of k_{RPM} in Fig. 7(a) was obtained using the algebraic equation (see Eq. (10)). The experimental reaction rate constants of the co-gasification char were higher than the calculated values. It indicates that there is a synergic effect between CC and BC co-gasification, which increased with the temperature at all mass ratios. The results of this study suggest that it is impossible to predict the reactivity of the blended char by using the additive equations (Eqs. (9)–(11)). Therefore, the synergic effect providing practical values of the gasification parameters are different from the linear superposition of separate gasification parameters. The influence of synergy on gasification parameters can be represented by the following expression (Eq. (12)):

$$V_{syn} = V_r - (F_1 V_{BC} + F_2 V_{CC})/(F_1 + F_2) \quad (12)$$

where V_{syn} is the synergistic effect parameter, V_r is the actual parameter during gasification, V_{BC} and V_{CC} represent the parameters of BC and CC, and F_1 and F_2 are the mass proportions of BC and CC in blends, respectively. Fig. 7(b) shows the influence of synergistic effect on the gasification activation energy, as expressed by Eq. (12). As the mass proportion of BC increases from 0% to 100%, the synergy activation energy E_{syn} has the maximum value at 75% BC mass proportion. This result is consistent with the optimum BC blending proportion concluded by the above-mentioned model analysis. However, the synergy, in terms of char gasification rate, was not observed in the previous study, although char was prepared from the rapid heating co-pyrolysis of rice straw and bituminous coal with a biomass and coal ratio of 1:1 [8]. It could probably be due to the relatively high pyrolysis temperature (1200°C), which leads to the loss of active surfaces and catalytic K species on the obtained char. Therefore, the obvious synergetic effect of the blended char may be caused by the following reasons: (1) compared with the morphological structures of BC prepared at 500°C [24], the initial morphological structures of char remaining after pyrolysis at 1100°C can maintain the diffusion rate of the gasifying agent [18]; (2) compared with BC or CC separate gasification, BC/CC co-gasification could decrease the uniformity, which made the experimental gasification rates of the co-gasification char higher than the calculated values [8].

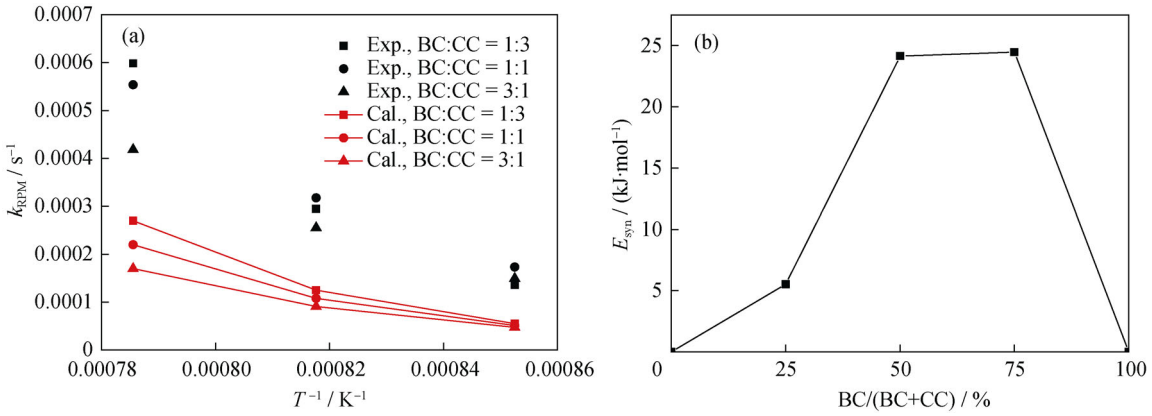

Fig. 7. (a) Comparison of K_{RPM} between calculation and experimental values; (b) influence of synergistic effect on E_{syn}.

5. Conclusions

The effects of blending ratio as well as gasification temperature on the char gasification characteristics were investigated using three kinetic models. The following conclusions can be obtained from this study.

(1) The gasification reactivity of the blended char improved with the increase of the BC share, and the gasification time was shortened. This result could be ascribed to the following two reasons: (i) higher specific surface area of BC and (ii) lower carbon structure uniformity of BC.

(2) When compared to VM and GM, the best model for describing CO_2 gasification of the blended char is found to be RPM, given the fact that only RPM can describe the phenomenon of an initial increase in conversion rate followed by a decrease. The activation energy of CC and BC, as determined by using the RPM model, was 210.2 kJ/mol and 126.7 kJ/mol, respectively.

(3) The activation energy is the minimum for the BC blending ratio of 75%. This is considered the optimum blending ratio for enhancing the gasification efficiency and carbon conversion rate. Synergy between CC and BC was also observed.

Acknowledgements

This work was financially supported by the National Natural Science Foundation of China (No. 51104014).

References

[1] J.S. Tao, The development of world DRI, [in] *China DRI Testing Seminar*, Tianjin, 2007, p. 126.

[2] Y.C. Shi, China's resources of biomass feedstock, *Eng. Sci.*, 13(2011), No. 2, p. 16.

[3] L. Dong, S.Q. Gao, W.L. Song, and G.W. Xu, Experimental study of NO reduction over biomass char, *Fuel Process. Technol.*, 88(2007), No. 7, p. 707.

[4] H.A. Long and T. Wang, Case studies for biomass/coal co-gasification in IGCC applications, [in] *ASME Turbo Expo*, Vancouver, 2011, p. 1.

[5] S. Li, X. Chen, L. Wang, A. Liu, and G. Yu, Co-pyrolysis behaviors of saw dust and Shenfu coal in drop tube furnace and fixed bed reactor, *Bioresour. Technol.*, 148(2013), p. 24.

[6] J. Fermoso, M.V. Gil, C. Pevida, J.J. Pis, and F. Rubiera, Kinetic models comparison for non-isothermal steam gasification of coal–biomass blend chars, *Chem. Eng. J.*, 161(2010), No. 1-2, p. 276.

[7] S. Krerkkaiwan, C. Fushimi, A. Tsutsumi, and P. Kuchontha, Synergetic effect during co-pyrolysis/gasification of biomass and sub-bituminous coal, *Fuel Process. Technol.*, 115(2013), p. 11.

[8] S. Yuan, Z.H. Dai, Z.J. Zhou, X.L. Chen, G.S. Yu, and F.C. Wang, Rapid co-pyrolysis of rice straw and a bituminous coal in a high-frequency furnace and gasification of the residual char, *Bioresour. Technol.,* 109(2012), p. 188.

[9] C. Gao, F. Vejahati, H. Katalambula, and R. Gupta, Co-gasification of biomass with coal and oil sand coke in a drop tube furnace, *Energy Fuels*, 24(2009), No. 1, p. 232.

[10] S. Kajitani, S. Hara, and H. Matsuda, Gasification rate analysis of coal char with a pressurized drop tube furnace, *Fuel*, 81(2002), No. 5, p. 539.

[11] K. Sangtong-Ngam and M.H. Narasingha, Kinetic study of Thai-lignite char gasification using the random pore model, *Thammasat Int. J. Sci. Technol.*,13(2008), No. 3, p. 16.

[12] G.G. Fouga, G.D. Micco, A.E. Bohe. Kinetic study of argentinean asphaltite gasification using carbon dioxide as gasifying agent, *Fuel*, 90(2011), No. 2, p. 474.

[13] H J. Mühlen, F. Sowa, and K.H. van Heek, Comparison of the gasification behaviour of a west and East German brown coal, *Fuel Process. Technol.*, 36(1999), No. 1-3, p. 185.

[14] M. Ishida and C.Y. Wen, Comparison of zone-reaction model and unreacted-core shrinking model in solid–gas reactions: I. Isothermal analysis, *Chem. Eng. Sci.*, 26(1971), No. 7, p. 1031.

[15] J. Szekely and J.W. Evans, A structural model for gas–solid reactions with a moving boundary, *Chem. Eng. Sci.*, 25(1970), No. 6, p. 1091.

[16] S.K. Bhatia and D.D. Perlmutter, A random pore model for fluid-solid reactions: I. Isothermal, kinetic control, *AIChE J.*, 26(1980), No. 3, p. 379.

[17] P. Ollero, A. Serrera, R. Arjona, and S. Alcantarilla, The CO_2 gasification kinetics of olive residue, *Biomass Bioenergy*, 24(2003), No. 2, p. 151.

[18] S. Yuan, X.L. Chen, J. Li and F.C. Wang, CO_2 gasification kinetics of biomass char derived from high-temperature rapid pyrolysis, *Energy Fuels*, 25(2011), No. 5, p. 2314.

[19] Y. Okumura, T. Hanaoka, and K. Sakanishi, Effect of pyrolysis conditions on gasification reactivity of woody biomass-derived char, *Proc. Combust. Inst.*, 32(2009), No. 2, p. 2013.

[20] K. Matsumoto, K. Takeno, T. Ichinose, T. Ogi, and M. Nakanishi, Gasification reaction kinetics on biomass char obtained as a by-product of gasification in an entrained-flow gasifier with steam and oxygen at 900–1000°C, *Fuel*, 88(2009), No. 3, p. 519.

[21] Y.T. Kim, D.K. Seo, and J. Hwang, Study of the effect of coal type and particle size on char–CO_2 gasification via gas analysis, *Energy Fuels*, 25(2011), No. 11, p. 5044.

[22] J. Deng, Y.H. Luo, Y.L. Zhang, and Y. Wang, Investigation into synergy in co-gasification of coal and char of biomass by thermogravimetric analysis, *J. Fuel Chem. Technol.*, 40(2012), No. 8, p. 943.

[23] C. Di Blasi, Combustion and gasification rates of lignocellulosic chars, *Prog. Energy Combust. Sci.*, 35(2009), No. 2, p. 121.

[24] Z.W. Hu, J.L. Zhang, H.B. Zuo, J. Li, Z.J. Liu, and T.J. Yang, Preparation and properties of biomass char for ironmaking, *J. Univ. Sci. Technol. Beijing*, 34(2012), No. 9, p. 998.